[논 문] 한국재료학회지
Kor. J. Mater. Res.
Vol. 18, No. 2 (2008)

DOI: 10.3740/MRSK.2008.18.2.061

Phase Change Characteristics of Sb-Based Phase Change Materials

Sung-Jin Park, In Soo Kim, Sang-Kyun Kim and Se-Young Choi†

School of Materials Science & Engineering, Yonsei University, 134 Shinchon-Dong, Seoul 120-749, Korea

(Received November 13, 2007 : Accepted December 20, 2007)

Abstract Electrical·optical switching and structural transformation of $Ge_{15}Sb_{85}$, $Sb_{65}Se_{35}$ and N2.0 sccm doped $Sb_{83}Si_{17}$ were studied to investigate the phase change characteristics for PRAM application. Sb-based materials were deposited by a RF magnetron co-sputtering system and the phase change characteristics were analyzed using an X-ray diffractometer (XRD), a static tester and a four-point probe. Doping Ge, Se or Si atoms reinforced the amorphous stability of the Sb-based materials, which affected the switching characteristics. The crystallization temperature of the Sb-based materials increased as the concentration of the Ge, Se or Si increased. The minimum time of $Ge_{15}Sb_{85}$, $Sb_{65}Se_{35}$ and N2.0 sccm doped $Sb_{83}Si_{17}$ for crystallization was 120, 50 and 90 ns at 12 mW, respectively. $Sb_{65}Se_{35}$ was crystallized at 170°C. In addition, the difference in the sheet resistances between amorphous and crystalline states was higher than $10^4\,\Omega/\gamma$.

Key words phase change materials, Sb-based materials, PRAM.

1. Introduction

Phase change materials, namely chalcogenides, show different properties at amorphous and crystalline states. These materials are applied to optical mass storage and phase-change random access memory (PRAM) by using their changes in optical and electrical properties upon phase transformation.[1-3] PRAM is one of the most promising candidates for the next generation nonvolatile memory devices. However, it still requires advanced materials, which exhibit low-power consumption, rapid phase transition and cyclic reliability. Recently, Sb-based materials have caught attention for the rapid crystallization behavior of Sb.[3-6] However, rapid crystallization would impede the stability of amorphous phase with unintended crystallization of amorphous recording. Thus, the main concern is to optimize the trade off condition between rapid crystallization and amorphous stability.[8-10] In this study, the main focus is on amorphizability, as a parameter to control the crystallization tendency, and Ge, Se or Si was employed as an amorphous stabilizer in Sb-based materials.

2. Experimental procedure

The films were deposited by radio frequency magnetron sputtering system (SNTek, Korea) on Si (100) wafers and slide glasses by using Ge (99.99%, RND KOREA, Korea), Se (99.997%, RND KOREA, Korea), Si (99.999%, RND KOREA, Korea) and Sb (99.999%, Kurt J. Lesker, U.S.A) targets. The base pressure was 5×10^{-7} Torr and working pressure was adjusted to 1 mTorr by introducing Ar at a rate of 10 standard cubic centimeters per minute (6N, Seoul gas, Korea) through mass flow controller. Targets were pre-sputtered for 5 minutes in order to remove oxidized surface and contaminations. Substrate holder was rotated at 20 rpm to obtain uniform thickness and homogenized composition of the films. Film composition was controlled by inducing different RF power to each target.

As-deposited films were annealed in Ar atmosphere for 10 min at 100~300°C with a heating rate of 5 K/min. The crystal structure was analyzed by X-ray diffractometer (Rigaku D/MAX II A, Japan & Philips X'pert MRD, Philips, Netherlands). The phase transition behavior on a nano-second scale was observed by laser irradiation using static tester (PST-1, Nanostorage, KOREA). Thickness of all films was 100 nm.

3. Result and discussion

3.1 Sheet resistance

Fig. 1 presents changes in the sheet resistances of Sb-based materials with different doping concentrations and annealing temperatures. At room temperature, all Sb-based materials were amorphous. The electrical switching of Sb-based materials was confirmed from phase transition.

†Corresponding author
E-Mail : sychoi@yonsei.ac.kr (S. Y. Choi)

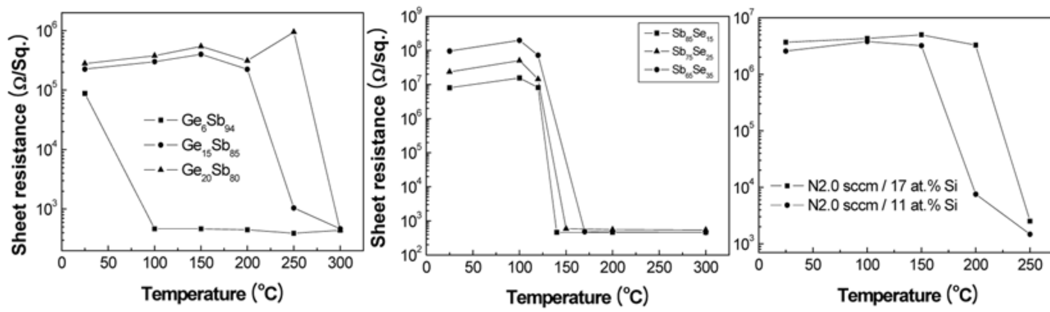

Fig. 1. Sheet resistance change of Sb-based materials with different doping concentrations and annealing temperatures.

In the case of Sb-Se alloys, large resistance margin between amorphous and crystalline states was observed. Especially, $Sb_{65}Se_{35}$ has the largest value of difference. The sheet resistance was 98 MΩ/□ at room temperature and decreased to 480 Ω/□ at 170°C. Such a decrease can be explained by the structural transformation of $Sb_{65}Se_{35}$. The sheet resistance of N2.0 sccm doped Sb-Si alloys at room temperature was about 5 MΩ/□. It decreased to 2 KΩ/□ after crystallization. In the case of 11at.% Si doped alloy, decrease in the sheet resistance occurred between 150°C and 250°C due to structural transformation. On the other hand, decrease in the sheet resistance of 17at.% Si doped alloy occurred between 200°C and 250°C. As the amount of Si increased, phase transition temperature increased and phase stability was also improved. In Ge-Sb alloys, difference in the sheet resistance varies with the doping concentration of Ge. As doping concentration of Ge increased, phase transition temperature increased. In addition, the margin of resistance between amorphous and crystalline states was increased. In PRAM, low phase transition temperature of phase change material may provoke unwanted phase transformation through thermal energy produced by the device operation. Therefore, phase transition temperature of around 200°C is suitable for PRAM application. For this reason, $Ge_{15}Sb_{85}$, $Sb_{65}Se_{35}$ and N2.0 sccm doped $Sb_{83}Si_{17}$ were chosen for our experiments.

3.2 Crystal structure

Fig. 2 shows XRD patterns of Sb and Sb-based materials with different doping concentrations and annealing temperatures. As-deposited Sb was crystalline and had hexagonal structure. XRD pattern of Sb annealed at 300°C exhibited Sb and Sb_2O_3 phases. As-deposited Sb-based materials are at amorphous states. Thus, it is possible to deduce that Ge, Se and Si might have reinforced the amorphous stability of Sb-based materials. $Ge_{15}Sb_{85}$ and N2.0 sccm doped $Sb_{83}Si_{17}$ were crystallized with heat treatment and have similar crystal structures with pure Sb. In the case of $Sb_{65}Se_{35}$, the 1st phase transition was observed at 170°C and the 2nd phase transition was observed at 280°C. At 280°C, the peaks can be identified as a mixture of Sb, Sb_2O_3 and Sb_2Se_3.

3.3 Crystallization behavior

To investigate the crystallization behavior in the scale of nano-seconds, static tester was employed. Fig. 3 indicates PTE (Power-Time-Effect)[6] diagram of Sb-based materials with changes in reflectivity. The reflectivity change, optical contrast (△,R) is defined by the following equation: △, R = $(R_{after}-R_{before})/R_{before}$, where R_{before} and R_{after} indicate the reflectivity before and after irradiation, respectively. The magnitude of R is illustrated by different colors in the PTE diagram. At low laser power and/or short pulse width (1st blue region), reflectivity does not change. When laser power and/or pulse width are increased, crystallization occurs. However, extremely high laser power and/or long pulsed width results in re-amorphization or ablation of the phase change materials (2nd blue region). An ablation is a kind of thermal destruction. In the case of $Sb_{65}Se_{35}$, relatively fast and easy crystallization occurred with short pulse width and/or low laser power. However, N2.0 sccm doped $Sb_{83}Si_{17}$ was hard to crystallize. Even at high laser power and long pulse width, ablation did not occur. It means that N2.0 sccm doped $Sb_{83}Si_{17}$ has a good thermal stability. $Ge_{15}Sb_{85}$ was very difficult to crystallize, while Ge_6Sb_{94} was easy to crystallize (not presented). Thus, high content of Ge impedes easy crystallization, which corresponds well with the result of changes in sheet resistance at different annealing temperatures.

Fig. 4 presents a nano-second scale crystallization behavior of $Ge_{15}Sb_{85}$, $Sb_{75}Se_{25}$ and N2.0 sccm doped $Sb_{83}Si_{17}$ at 6, 12, and 18 mW, respectively. Reflectivity

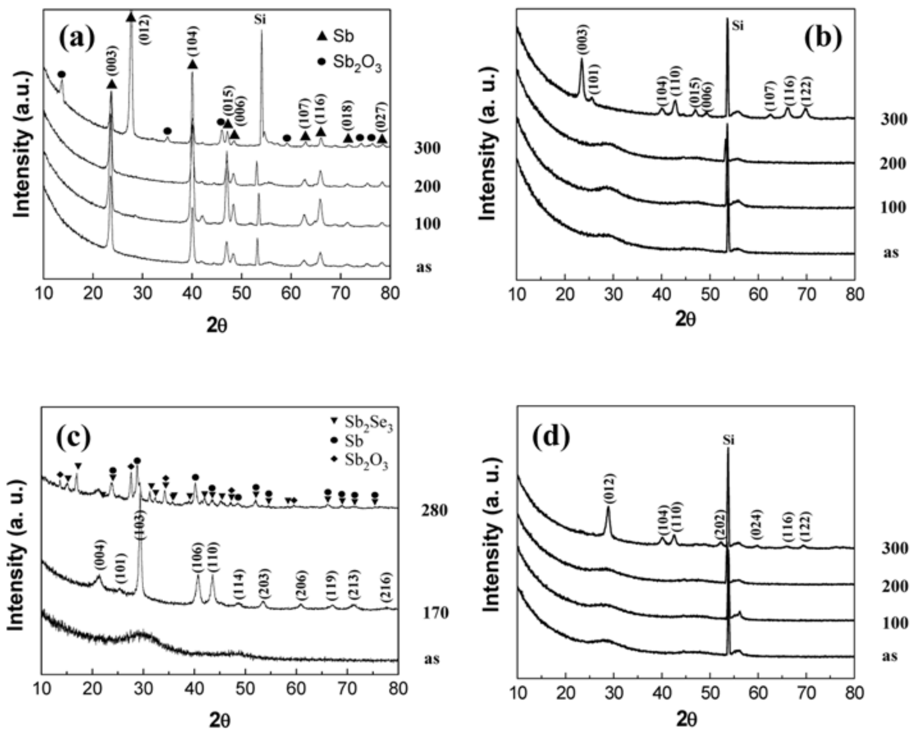

Fig. 2. XRD patterns of (a) Sb, (b) $Ge_{15}Sb_{85}$, (c) $Sb_{65}Se_{35}$ and (d) N2.0 sccm doped $Sb_{83}Si_{17}$ annealed at different temperatures.

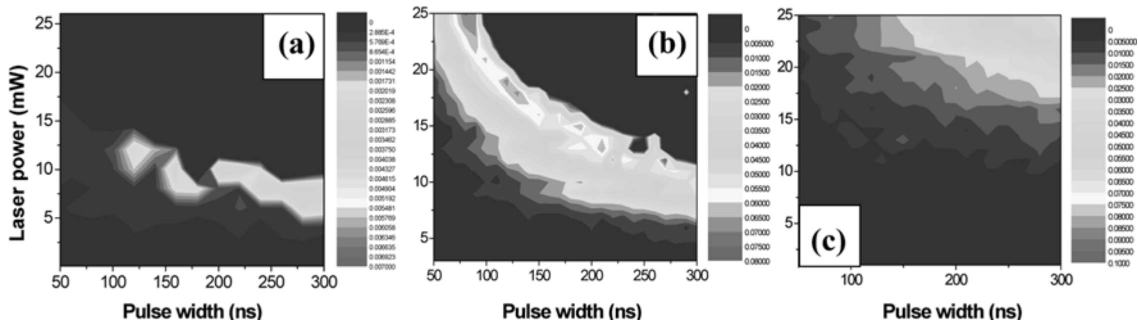

Fig. 3. PTE(Power-Time-Effect) diagram of (a) $Ge_{15}Sb_{85}$, (b) $Sb_{65}Se_{35}$ and (c) N2.0 sccm doped $Sb_{83}Si_{17}$ with reflectivity changes.

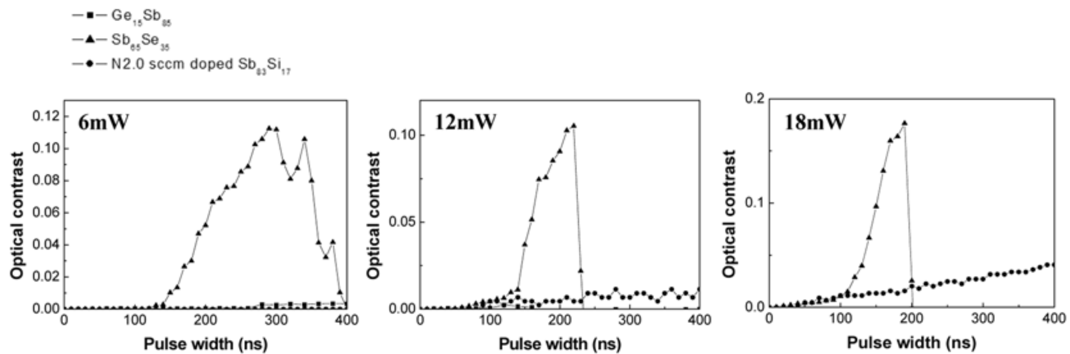

Fig. 4. Nano-second scale crystallization behavior of $Ge_{15}Sb_{85}$, $Sb_{65}Se_{35}$ and N2.0 sccm doped $Sb_{83}Si_{17}$ with different laser power and pulse width.

changed due to crystallization and ablation. In the case of $Ge_{15}Sb_{85}$, at 6 mW, the minimum time for crystallization was 280 ns and ablation did not occur. At 12 mW, crystallization started from 120 ns and ablation was observed at

180 ns. At 18 mW, only ablation occurred. The minimum time for crystallization of $Sb_{65}Se_{35}$ was 120, 50 and below 10 ns at 6, 12 and 18 mW, respectively. The ablation of $Sb_{65}Se_{35}$ appeared at 300, 230 and 190 ns with 6, 12 and 18 mW, respectively. From the results, $Sb_{65}Se_{35}$ can be taken as a material exhibiting rapid phase transformation and low power consumption during device operation. Therefore, $Sb_{65}Se_{35}$ is an effective candidate for PRAM application. The minimum time for crystallization of N2.0 doped $Sb_{83}Si_{17}$ was 420, 90 and 50 ns at 6, 12 and 18 mW, respectively. As it could be seen from fig. 3, it doesn't have ablation region under 45 mW laser power and/or 450 ns pulse width. From this result, we can deduce that N2.0 doped $Sb_{83}Si_{17}$ is a powerful candidate as a material of enhanced phase stability.

4. Conclusion

Ge, Se or Si led to higher crystallization temperature, meaning that Ge, Se and Si might have acted as amorphous stabilizers. $Sb_{65}Se_{35}$ showed rapid and easy crystallization. In addition, it had higher sheet resistance in amorphous state and showed higher difference in sheet resistance than $10^4\Omega/\square$. $Ge_{15}Sb_{85}$ and N2.0 sccm doped $Sb_{83}Si_{13}$ were hard to crystallize by laser irradiation. Moreover, those alloys have lower difference in sheet resistance than $10^4\Omega/\square$. Therefore, $Sb_{65}Se_{35}$ is expected to show good device operation.

Acknowledgement

This work was supported by the Second Stage of Brain Korea 21 Project in 2007.

Reference

1. J. Feinleib and S. R. Ovshinsky, J. Non-Cryst. Solids **4**, 564 (1970).
2. N. Yamada, E. Ohno, K. Nishiuchi, N. Akahira and M. Takao, J. Appl. Phys. **69**, 2849 (1991).
3. J. Solis, C. N. Afonso, S. C. W. Hyde, N. P. Barry, and P. M. W. French, Phys. Rev. Lett., **76**, 2519 (1996).
4. K. Ito, H. Tashiro, M. Harigaya, E. Suzuki, K. Tani, N. Yiwata, N. Toyoshima, K. Makita, A. Kitano and K. Kato, Mater. Res. Soc. Symp. Proc., **803**, HH5.2.1, ed. L. Hesselink and A. Mijiritskii, Mater. Res. Soc., Pittsburgh, USA (2004).
5. J. P. Callan, A. M. T. Kim, C. A. D. Roeser and E. Mazur, Phys. Rev. Lett., **86**, 3650 (2001).
6. M. J. Kang, S. Y. Choi, D. Wamwangi, K. Wang, C. Steimer and M. Wuttig, J. Appl. Phys., 98, 014904 (2005).
7. L. Pieterson, M. Schijndel, J. C. N. Rijpers and M. Kaiser, Appl. Phys., Lett. **83**, 1373 (2003).
8. J. Solis, C. N. Afonso, J. F. Trull and M. C. Morilla, J. Appl. Phys. **75**, 7788 (1994).
9. R. Bez and A. Pirovano, Mater. Sci. in Semiconductor Processing, **7**, 349 (2004).
10. N. Yamada, E. Ohno, K. Nishiuchi, N. Akahira and M. Takao, J. Appl. Phys., **69**, 2849 (1991).